

Semiconductor Interfaced Biosensor

Ming Rui Zhang*

The university of Manchester, Manchester, UK.

* Corresponding author. Tel.: 15509822848; email: mingrui.zhang-2@student.manchester.ac.uk

Manuscript submitted July 3, 2020; accepted September 19, 2020.

doi: 10.17706/ijbbb.2020.10.4.180-192

Abstract: Semiconductor (SC) based field-effect transistors (FETs) have been demonstrated as an elite enhancer gadgets particularly their high delicate interface towards the surface adsorption, which lead wide application as sensor and biosensors. Be that as it may, traditional planned structures are enduring the low selectivity and significant expense, representing a significant boundary to down to earth application for the clinical finding. Presently the plan dependent on semiconductor material is considered for fitting wearable biosensor applications because of the fast reaction time for constant and consistent observing, enormous recognizable fixation extend, high affectability, high consistency for solid detecting, and the capacity to coordinate with other microfluidic and electronic practical gatherings. This survey abridged the latest advances in this field, which address ebb and flow difficulties in biosensor examine. The work pointing the further advancement and explicit applications for which these trademark properties become one of a kind (i.e., not effectively accomplished by different materials) have been reviewed here. Through solid requests for research and thought of sensor application, it will have the option to move the innovative sensor with the extraordinary semiconductor interface structure.

Key words: Biosensor, semiconductor, field effect transistor.

1. Introduction

Semiconductor based field-effect transistors (FETs) have pulled in critical consideration because of their high delicate interface with fluid, which make them viable as biosensors. Semiconductor additionally has a few qualities, for example, warm affect ability, photosensitivity, negative resistivity temperature, rectifiable, etc. In this manner, semiconductor materials can be utilized for control gadgets, optoelectronic gadgets, pressure sensors, thermoelectric refrigeration and different applications other than assembling enormous scale coordinated circuits. There are numerous orders for sensors, yet there are two usually utilized groupings: one is arranged by the deliberate physical amounts, the other is characterized by the working rule of sensors. Sensors arranged by estimated physical amounts are usually temperature sensor, moistness sensor, pressure sensor, uprooting sensor, stream sensor, fluid level sensor, power sensor, speeding up sensor, torque sensor, and so on.

Nanobiosensors dependent on semiconductor material are appropriate for wearable biosensor applications on account of the speedy reaction time, enormous perceivable fixation run, high affect ability, high consistency for solid detecting, and the ability to coordinate with other microfluidic and electronic useful groups.¹ Especially, one-dimensional (1D) nanomaterials have huge surface-to-volume proportions and tunable physical properties. These qualities can be utilized to accomplish better execution over mass materials in an assortment of utilizations, including hardware, optics and photonics, vitality stockpiling and

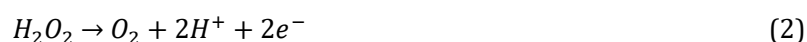
change gadgets, natural and concoction sensors, intracellular conveyance of bioactive atoms, and restorative gadgets. As of now, another class of natural semiconductor gadgets functionalized by the quick ionic movement in the room temperature liquid salts was uncovered. This new sort of strong to-fluid interface is framed between natural semi-conductor single precious stones and ionic fluids so that the structures fill in as quick exchanging natural field-impact transistors OFETs with the most noteworthy transconductance $gm = ID/VG$ per square channel sheet, i.e., the most proficient reaction of the yield channel current ID to the information entryway voltage VG among the OFETs at any point constructed. OFETs are possibility for cutting edge minimal effort de-indentencies that can be created by straightforward manufacture forms [1]. Be that as it may, Performance is constrained by poor authority over the quantities of utilitarian nanowires present in gadgets. top-down systems experience the ill effects of significant gear and use costs. In late years, the interest for profoundly touchy and reusable biosensors has expanded in light of the fact that the applications dependent on biosensors have gotten different, with the range including medicinal, rural, modern, and ecological fields [2].

2. Inorganic Semiconductor/Aqueous Interface

2.1. Nano FET Biosensor

2.1.1. On-chip metal electrode

For the biosensor application, other than blood, other organic liquids, for example, sweat, tears, and spit likewise contain gigantic biochemical analytes that can give significant data and are all the more promptly available contrasted with blood. Contrasted and the combination of the Ag/AgCl terminal into a biosensor chip which stays testing. For PET-based biosensors, the entryway anode just needs to supply stable door inclination to the gadgets, which can be accomplished by an on-chip metal side cathode. The creators as of late exhibit a profoundly touchy and conformal In_2O_3 nanoribbon FET biosensor with a completely coordinated on-chip gold side door, which have been overlaid onto different surfaces. They have added side entryway examples to the source/channel shadow cover and have utilized a $5\ \mu m$ ultraflexible PET substrate and the subsequent shadow veil was then overlaid onto the PET substrate for the accompanying metal statement. Besides, the chitosan ink was imprinted on PET In_2O_3 and the source and channel cushions utilizing an inkjet printing procedure. Also, the gold side door was utilized rather than Ag/AgCl anode which expands the means and trouble of creation. For affirming the detecting capacity of biosensor the creators test the ionic affect ability of the biosensor chip with a gold side or an Ag/AgCl cathode by PH detecting test [3].



2.1.2. In_2O_3 nanoribbon arrays

The Johnson group report on the creation of huge region In_2O_3 nanoribbon exhibits utilizing CLL, yet without utilizing bosses produced by means of EBL. The gathering utilized HD-DVDs as bosses for CLL PDMS stamps. These stamps are reusable and can be utilized for rehashed, wafer-scale CLL designing. Nuclear power micrographs of designed PDMS surfaces affirmed exact replication of HD-DVD highlights with profundities of $\sim 60\ nm$. Filtering electron microscopy of CLL-designed SAMs affirmed the nearness of 1D highlights ($200\ nm$ linewidths) over huge zones, coordinating those on the stamps. The widths ($\sim 200\ nm$) and statures ($\sim 3\ nm$) of the metal oxide nanoribbons are the littlest, as far as anyone is concerned, created by means of top-down approaches. To assess the exhibition of In_2O_3 in gadgets, the gathering built FETs in a

base door, top-contact arrangement. 3000 200-nm-wide In_2O_3 nanoribbon were consolidated into every FET device. They exhibit superior FETs created utilizing In_2O_3 nanoribbons having transporter mobilities up to $13.7 \text{ cm}^2 \text{ V}^{-1} \text{ s}^{-1}$ and on/off current proportions >10 (Fig. 1). These nanoribbon FETs have comparable electronic properties to In_2O_3 slim film transistors, however have higher surface-to-volume proportions. The presentation of these gadgets, for example, current on/off proportion, surpassed those recently detailed for 1D nanowire-based gadgets manufactured by means of base up approaches. The nanostructures, for example, In_2O_3 nanoribbons and others, will be helpful in nanoelectronics and biosensors. The method showed here will empower these applications and grow minimal effort, huge zone designing methodologies to empower an assortment of materials and structure geometries in nanoelectronics [4].

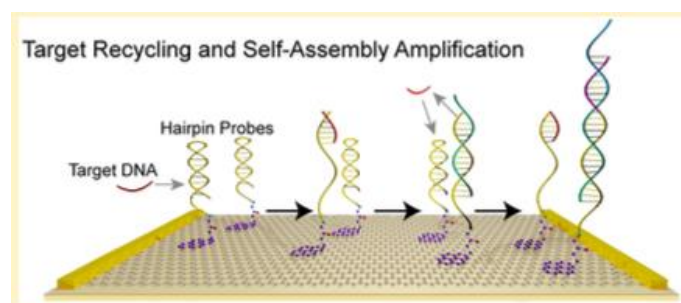


Fig. 1. Target recycling and self-assembly amplification.

2.1.3. Self-assembled graphene field-effect biosensors

The Johnson report a method to overcome the length dependent property of GFET DNA corrosivity sensor which depends on single strand DNA testing. Their test shows that compared with the traditional single strand DNA testing, the clasp DNA testing has a higher specificity for non complete DNA. They show multi-channel positioning using GFET clusters. An optical image of a GFET display manufactured using the applicable lithography process described in the materials and methods section. Soon, a large area of graphene ($10\text{cm} \times 15\text{cm}$) was incorporated into the copper foil through the low-pressure mixing smoke affidavit, and transferred to the Si / SiO_2 substrate through the recently manufactured Cr / Au anode. GFETs were functionalized by incubation with 1-pyrenbutyric acid (pbase) in N, N-dimethylformamide (DMF). After functionalization, GFETs were incubated with water sample array of aminated DNA fragments. Barrette test DNA is metastable and can be opened explicitly by the target DNA, thus triggering the self aggregation reaction. In the $5\times$ sodium citrate (SSC) hybrid vector, GFET biosensor clusters were mixed with known target DNA in the presence of H2, H3 and H4 (all with a convergence of $1 \mu\text{m}$), and I-Vg properties were estimated in the dry state (Fig. 2).

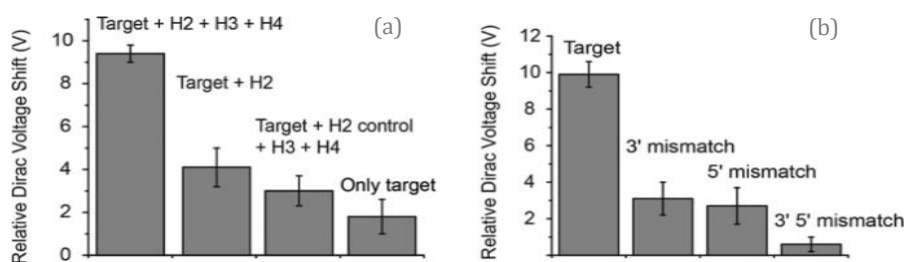


Fig. 2. Biosensor response to positive and negative controls. (a) Relative Dirac voltage shifts for various positive control experiments based upon concentrations of $1 \mu\text{m}$ for the target DNA and the specified helper DNAs. (b) Relative Dirac voltage shifts for 10 nm target DNA and negative controls with base mismatches at the ends. Error bars are standard deviation of the mean. Helper DNAs were of $1 \mu\text{m}$.

In order to explain the factors of self-polymerization amplification, a scientific model is established, which reflects the key biochemical reaction, which connects the target DNA oligomer to the start of amplification reaction mediated by cyclase H1 and H2. The model also anticipates that exploratory dose-response bending is an element of incubation time: at low targets (fm-run), considering that the target DNA reused will open additional H1 bands over time, thus increasing the number of H1, H2, H3, H4 buildings, it is expected that Dirac voltage movement will develop if the test is conducted in a longer time (> 1 hour). The model is expected to be approved temporarily (Fig. 3). Under the same experimental conditions, the incubation time was extended to 100h instead of 1h by three methods (100pm, 100fm, 100am). The biosensor was immersed in 1h and the polymerization degree was 100 pm. For the lower focal length (100fm, 100am), the reaction will gradually expand after a period of time. In order to verify the feasibility of identification methods based on target reuse and self-aggregation enhancement, GFET experiments were carried out on some positive controls [5].

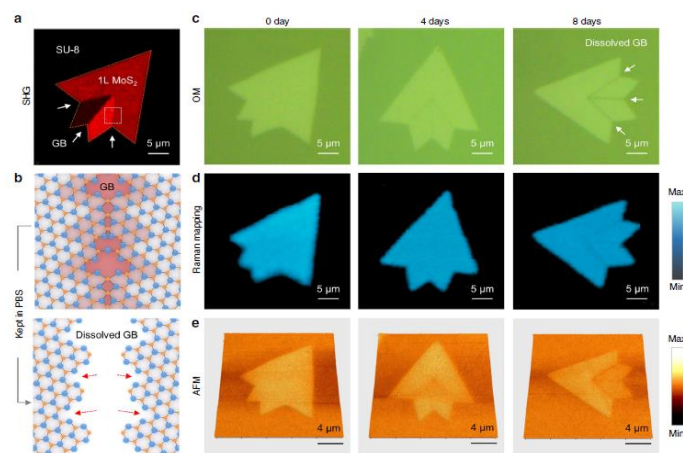


Fig. 3. Morphological and structural evolution of isolated monolayer MoS₂ crystals with different dissolution times in PBS solution. a SHG image of an APCVD-grown polycrystalline monolayer MoS₂ crystals on an SU-8/sapphire substrate, showing the distribution of GB regions. b Schematic illustration of the MoS₂ GB marked in the dotted box of (a) before and after dissolution in PBS solution. C-e OM (c), Raman A1g intensity mapping (d), and AFM (e) images of monolayer MoS₂ crystals, immersed in a PBS solution (pH 7.4) at 75 °C with different dissolution times (0-8 days).

2.1.4. Monolayer MoS₂ interface

The Chen gathering report the disintegration qualities and conduct of both confined precious stones and constant movies of CVD-developed monolayer MoS₂ in phosphate cradled saline (PBS) arrangements at different temperatures and with various pH levels. To show a few potential outcomes in superior gadgets, Chen created MoS₂-based bioabsorbable, multifunctional sensors with abilities for estimating pressure, temperature, strain, and quickening and the outcomes propose that presentation of 2D semiconducting materials into transient electronic frameworks may prompt noteworthy open doors in the advancement of adaptable, stretchable, conformal, and straightforward gadgets and frameworks with insignificant materials load on the earth or potentially encompassing science. To uncover the science and concoction energy of disintegration of monolayer MoS₂ in PBS arrangement, the Chen bunch originally explored secluded precious stones with few grain limits (GBs). The general end is that disintegration of monolayer MoS₂ precious stones in PBS happens as an imperfection actuated scratching process. Because of the diminished dynamic vitality hindrance, the MoS₂ GBs break down first, trailed by point imperfections, and afterward locales that reach out along the flat course opposite to the messed up edges, in the end combining and prompting total

disintegration and the absolute disintegration time can be diminished with littler grain size, in this way giving a way to deal with tuning the lifetime of bioabsorbable electronic gadgets. Low-pressure concoction fume affidavit (LPCVD) gives a versatile way to orchestrating such films (for more data on this procedure, kindly allude to the Methods Section). With a seed layer, enormous scale, constant movies of MoS_2 can be developed on SiO_2/Si substrates (Fig. 4).

Chen's collective studied the cytotoxicity of MoS_2 during the disintegration process, using the starting material of continuous film, the separated chip, and the pre decomposition in PBS arrangement, and then analyzed the long-range biocompatibility of MoS_2 membrane in vitro. As well as the non-toxic nature of instantaneous MoS_2 Bioelectronics, the rationality of its long-term use in human body is recommended. These findings about the biocompatibility and bioabsorbability of MoS_2 make it applied in implantable and short biomedical sensors. Chen collected and described many MoS_2 based bioabsorbable sensors, which are used to accurately estimate weight, temperature, strain and motion. The sensors implanted in the intracranial space of the biological model (mouse) allow to display the important utilization methods of observing patients in the rehabilitation period after the extremely terrible mental injury (Fig. 5). The results show that the results of continuous in vivo examination and traditional small tools of organic markers by fully bioabsorbable sensors.



Fig. 4. Optical images of a MoS_2 -based bioabsorbable sensor implanted in a rat together with a commercial one before and after suture.

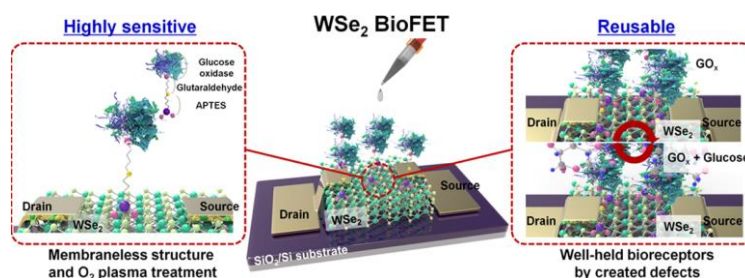


Fig. 5. Membraneless field-effect transistor (FET)-type tungsten diselenide (WSe_2) biosensors.

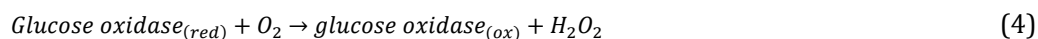
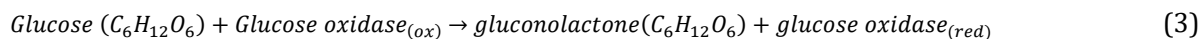
2.2. Membraneless FET Biosensors

Parker's gathering showcases an extremely refined, reusable, film-free biofilm of tungsten diselenide (WSe_2), one of the channeled materials, WSe_2 , which has a layered structure of progressive metal dihalides dependent on van der Waals (VDW) interactions. 1. There is no catenary bond deformation on the surface of WSe_2 , considering the deep touching activity of the membraneless WSe_2 biofilm. Not subject to fuzzy authority. We extended the falsifiability of WSe_2 biofilms by generating a small number of defects on the non-defective WSe surface as a restrictive destination for the biological receiver.

They treated WSe_2 slices of silicon dioxide/silicon substrate with oxygen plasma for 15 and 30 seconds. As indicated by these XPS results, aggregation speculates that O_2 plasma treatment destroys the security of WSe , thus generating Se opportunities and W-O bonds on the surface of WSe_2 . The biological receptor (glucose

oxidase: GO) was fixed on the surface after WSe₂, O₂ plasma treatment. We arranged the control, 15 and 30s plasma treatment WSe₂ test and incubated the example in the APTES response for 30 minutes. Fill in the form of a synthetic linker to anchor the GOx biosector atoms to the WSe₂ biosensor. Due to the W-O safety after oxygen plasma treatment, more and more aptes atoms are dependent on being connected to the surface of WSe₂ as silane binds well to the oxygen-rich surface.

In order to explore the detection method of WSe₂ biofilm without membrane, aptes, glutaraldehyde (central connector) and go (the last biofilm) were used to perform surface functionalization treatment on WSe₂ biofilm treated by O₂ plasma. The non-membrane WSe₂ biofilm was tested and rinsed with glucose for more than one time to analyze its reusability [6].



2.3. Photoelectrochemical Biosensors

In photoelectrochemistry, light is utilized to produce electron/opening sets in a photoactive material, and these electron/gap sets, when isolated, are utilized to drive redox responses. Contingent upon the responses happening in the photoelectro-compound (PEC) cell, light is then changed over to electrical or synthetic energy. Recently, PEC signal transduction has been exhibited for organic detecting. In PEC biosensors, light is utilized to create charge transporters in photoactive materials, and the transduced electrochemical current is estimated for examining naturally significant targets. Since signal readout is electrochemical, this technique acquires the advantages of electrochemical biosensing:

- (1) the sign is perused utilizing economical and simple to-utilize instrumentation.
- (2) multiplexed location is accomplished utilizing multielectrode microchips.
- (3) Due to optical excitation, PEC estimations are performed at lower inclination possibilities contrasted with their electrochemical partners.
- (4) this brings down the deliberate electrochemical foundation flows and builds the sign to-foundation proportion. PEC readout has been utilized to identify biomolecules, for example, DNA, RNA, and proteins.

In any case, when utilizing these creation techniques, an exchange off must be made between the level of auxiliary tunability, throughput, and cost.

The gathering utilized surface wrinkling to upgrade the proficiency of photocurrent age in detecting PEC cells. Surface wrinkling is a simple and economical technique for bringing tunable smaller scale and nanostructuring into dainty movies, permeable systems, and get together of nanoparticles. In this work, they made a strategy for stacking photoactive QDs into a wrinkled platform of a straightforward conductive oxide to improve the produced photocurrent. By functionalizing the photoactive QDs implanted in the wrinkled film, we built up a sensor for distinguishing DNA targets. The wrinkles were made legitimately on polystyrene by shaping a hardened oxidized surface layer and contracting the substrate. The ITO and QDs were then sputtered and stacked into the wrinkled polystyrene framework, separately. The distinctions in surface geology and progression between the three classes of photoelectrodes. The standard photoelectrodes are planar, and their ITO layer was free of breaks. These components, which the article talked about, additionally empowered the oxidized layer to adjust instead of break in light of the applied strain, making a nonstop wrinkled layer and afterward PEC current for the scaffolded-wrinkled surface (at 3 layers) was around multiple times bigger than the current accomplished in the planar surface. Stem was utilized to think about PEC current pattern and as the charges travel through the system of QDs and the PDDA spacer, resistive misfortunes, dispersion misfortunes, and recombination decline their gathering rate by the ITO anode,

further lessening the photocurrent (Fig. 6). The gathering explored the progressions in PEC current when the scaffolded-wrinkled photoelectrodes were interfaced with test and target DNA strands. The upgraded PEC current acquired utilizing the wrinkled materials design empowered us to build up a delicate and mark free DNA biosensor with a picomolar limit-of-detection [1].

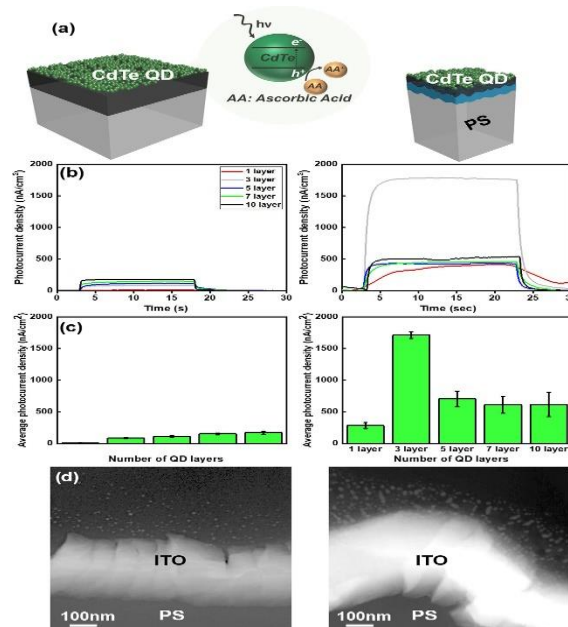


Fig. 6. PEC measurements at planar and scaffolded-wrinkled photoelectrodes. (a) Visible light (470 nm) induces electron/hole pairs in CdTe QDs. Holes oxidize ascorbic acid, generating an anodic redox current. (b) PEC current densities measured on planar (left) and scaffolded-wrinkled (right) devices using 100 mM ascorbic acid at 0 V with respect to Ag/AgCl. The QD layers are increased by depositing alternate layers of QDs and poly (diallyldimethylammonium chloride) (PDDA). The 470 nm light-emitting diode is turned on at 3 s and turned off at 23 s. (c) The average PEC current densities measured on planar (left) and scaffolded-wrinkled (right) devices for different numbers of QD layers. (d) Scanning transmission electron micrographs of cross sections of planar (left) and scaffolded-wrinkled (right) devices. The imaged devices contain three QD layers.

2.4. Nano Optical Biosensor

Nano-silicon photonics is an ideal stage to realize high orthodontic and selective recognition of organic atoms under complex fluid conditions. In this case, luminescent silicon-based nanostructures are very encouraging materials because their large uncoated surfaces and their optical properties are due to the most innovative conduction techniques. In the aspect of DNA recognition, the basic detection of Si-nws was carried out by using the electric conduction strategy based on DNA hybridization conductance variation and the explicit detection method fixed on the surface of NWS, and 220 atom (about 6600 DNA target duplicates per 50 μl) low fracture points were found. SSDNA, by using a variety of crystal silicon nano-field effect transistors (FET) with measurements of less than 20nm, another interesting approach relies on fluorescent labeling of DNA. In particular, his collection demonstrates the high performance of Si NWs biochemical sensors to reduce the identification of various named genome sequences to as low quality as possible. Sabrin's collection reported major cases of direct genomic identification in Si-NWs optical biosensors without enhancement steps (sans-pcr) and without markers (unlabeled). The proposed approach utilizes a hybrid approach that combines Si NWS with satisfactory in situ hybridization from two explicit experiments

and synthesizes it on the surface with a genomic double strand. We tried to show sensors that take advantage of the hepatitis b virus (HBV) genome.

Pleasant to confirm the adequacy of the hybrid as optimal capture component, sabrinas before collection through specific Raman measurement tried real proximity of HBV genome, we also observed the NWS sensor with HBV (blue line) the vibration of the sample, the NWS sensor range of Raman and thrown into the Si substrate and then dry like drops of Raman scope of the same DNA. So the sabrina family gathering could feel the same spectral commitment, although in the NWS sensor, the Raman signal from HBV's better features was affected by the slight movement of the Raman group and the different relative force ratios, which led to the gradual convolution of spectral highlights. To further assist in the Raman characterization of DNA captured by our silicon nanosensors, attenuated total reflection infrared spectroscopy (atr-ir) analysis was performed (Fig. 7). After showing HBV DNA capture, they tried the sensor by estimating changes in light outflow as part of a repeat/response. To verify the accuracy of the obtained results, we performed simple pl estimates on five silicon nanosensor to demonstrate the repeatability of the results. The synergistic effect of HBV and functionalized NWS determines the termination of this gene symbol is used as the identification instrument.

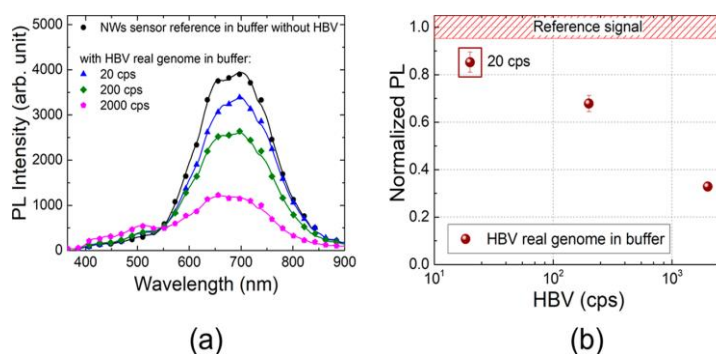


Fig. 7. (a) PL spectra of the NWS sensor tested in HBV real genome extracted from infected human blood and spiked in buffer reported for different concentrations ranging from 20 cps up to 2000 cps. The PL reference of the sensor without any copies of HBV is shown in black. (b) Trend of the PL integrated peak of the deconvolved NWS PL emission as a function of real HBV genome concentration normalized to its reference signal (red bar) obtained by the buffer solution without any real HBV copy. The quenching of the PL signal used as detection mechanism.

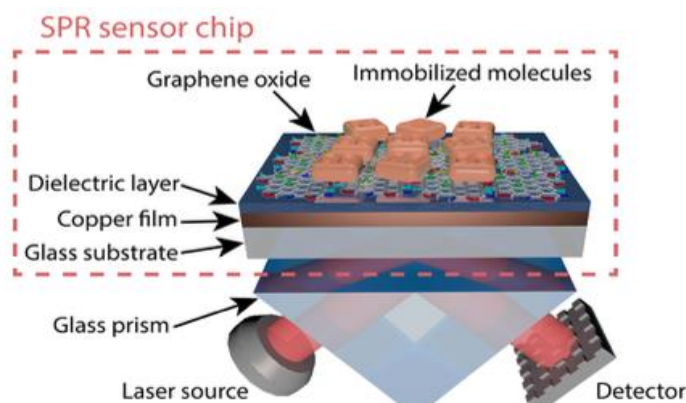


Fig. 8. Schematic representation of the SPR biosensor comprising the SPR sensor chip based on plasmonic copper films coated with a dielectric layer to protect against oxidation. The prism and sensor chip substrates are made of the same type of glass, which allows for an efficient optical connection. The immobilization of biomolecules on the biosensor surface can be achieved using a graphene oxide linking layer deposited atop the dielectric layer.

The impact of a natural network and its potential impedances can be evaluated by testing the Si NWs sensor with HBV clone genome broke up in human serum rather than the support arrangement. To affirm this theory, a Si wafer (without NWs) was tried with an answer made by human serum without HBV and a similar wide multipeaked band 400-600 nm was watched and was plainly verify that the PL signal variety of the NWs sensor as a component of HBV focus is the equivalent in the two grids (Fig. 8). The presentation evaluation of the Si NWs sensor with genuine examples is a significant point to be tended to. To further explore this point, we tried the gadget by utilizing a genuine HBV genome removed from a blood test. It was affirmed that this Si NWs sensor can distinguish the genuine HBV genome separated from human blood with an effectiveness similar to the constant PCR (20 cps/response), regardless of whether its length is about portion of the analytical sample [7].

3. Metal-Assisted Interface

Plasma biosensors are widely used in logic and medicine research, medical diagnosis, veterinary practice, nutrition and health control. Stebunovs collects copper as a plasma material for constructing biosensor interfaces. One potential way to overcome this problem is to protect the hidden metal surface with a graphene-covered barrier, while having a negligible effect on the optical properties of the interface between the sensor surface and the substance to be tested or the organic frame. Stebunovs' team proposed the SPR sensor chip, which relies on plasma-copper membranes fixed with different dielectric layers (Fig. 9). The disappearance of the electron column is an essential part of the standard cmos process, which stores thin copper film on the surface of the glass substrate. The optical properties of the metal film determine the probability of SPR excitation in a specific structure, the reverberation quality and the feasibility of SPR biosensors. The ellipsoidal model shows that the dielectric constants of copper and gold films are directly determined by the ellipsoidal information. The RI variation of copper SPR sensor chip with different protective layers is hypothesized and preliminarily tested. Improvement with ligand specific interface is SPR biosensing applications analysis is an important part of because graphene material with large surface area and different material properties, the interface can be applied to a wide range of biological chemical association study, no matter under what circumstances, compared with sulphur connection layer, increase the limit immobilized. For the first time, we show the progress of the go connection layer covering the dielectric layer outside the SPR biosensor chip [7].

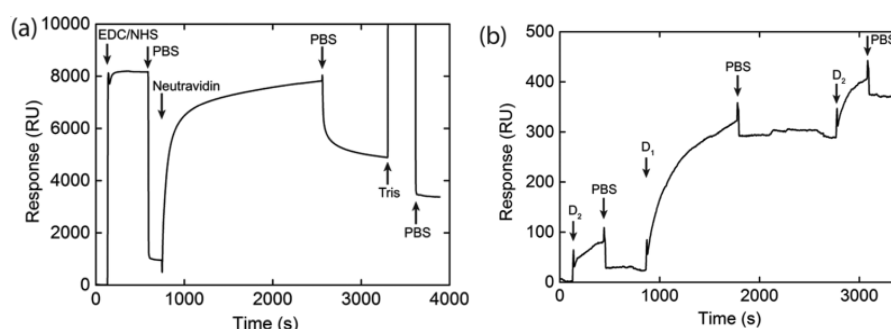


Fig. 9. (a) Covalent immobilization of neutravidin on the surface of the graphene oxide (GO) linking layer deposited on the copper surface plasmon resonance (SPR) sensor chip protected by 15 nm thick Al_2O_3 film. Immobilization procedure includes the activation of carboxyl groups of GO by the mixture of 0.4 M 1-ethyl-3-(3-(dimethylamino) propyl) carbodiimide hydrochloride (EDC) and 0.1 M N-Hydroxysuccinimide (NHS) solutions and deactivation of carboxyl groups after neutravidin adsorption by 1 M Tris solution. (b) Adsorption of oligonucleotides D1 and D2 on the surface of neutravidin-GO copper SPR chip. D1 is biotinylated and complementary to non-biotinylated D2. PBS: phosphate-buffered saline.

4. Inorganic Semiconductor/Ionic Liquid Interface

4.1. What Is Ionic Liquid and What Is Its Properties

According to the specific material framework, various strategies are used to create extremely light crystalline layers, including various stripping methods and material manufacturing methods. These programs play a very good role in most van der Waals layered materials, because the absence of covalent bond between adjacent layers improves the strength of the mixture, and eliminates the problems caused by the hanging bond on the surface of the material, so that the thickness of the "defect free" gem is reduced to the core thickness. The results show that the electronic properties of the materials can be quantitatively measured by the ion fluid gate field effect transistor (FET) which is prepared on the large drop point gem. WS_2 is a kind of ring gap semiconductor (ΔWS_2 1.35eV), which consists of two-dimensional (2D) covalently enhanced S-W-S layer and van der Waals gap isolation (Fig. 10). It is found that by coupling WS_2 microchip with ionic liquid medium, stable, non sluggish, electronic and gap conductance adjustable bipolar transistors can be obtained. It can be imagined that the band gap of WS_2 can be reasonably determined with high accuracy (10%) by the dependence of the current active channel's input voltage, and the careful use of the ion fluid gate transistor provides an incredible asset for the quantitative study of the electronic characteristics of fragile gemstones.

Slim crystalline pieces of WS_2 were gotten by mechanical peeling of a mass single precious stone developed by synthetic fume transport and afterward moved on an exceptionally doped Si/SiO₂ substrate. Chips appropriate for electrical portrayal were distinguished under an optical magnifying lens and their thickness was estimated by atomic force microscopy (AFM). Electrical contacts were manufactured by electron-bar lithography, trailed by metal (Ti/Au) dissipation and lift-off. The gadget yield attributes, estimated for the two polarities of VG and VD, affirm the high-caliber of the ambipolar transistor activity (Fig. 11). The gathering can absolutely decide the band gap of WS_2 from basic vehicle estimations on a nanofabricated FET and ionic liquid gated FETs made on WS_2 slim drops are demonstrated to be perfect ambipolar gadgets on account of an essentially ideal electrostatic coupling between the ionic fluid door and the transistor channel and to the high caliber of the utilized semiconductor [8].

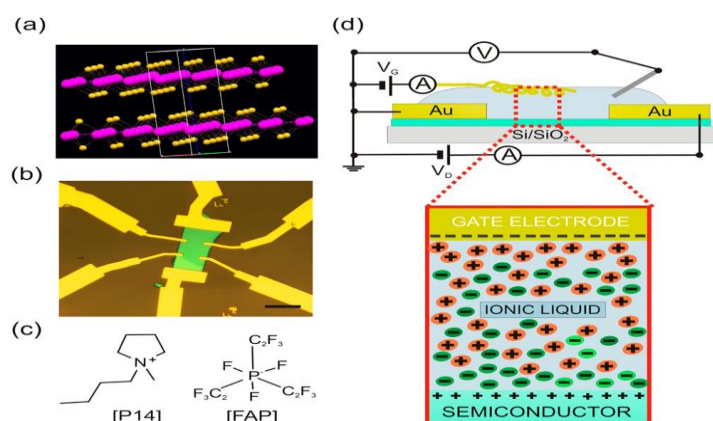


Fig. 10. (a) Crystal structure of layered WS_2 ; the purple balls correspond to W atoms and the yellow balls to S atoms. (b) Optical microscope image of a six-terminal Hall bar fabricated on a crystalline WS_2 thin flake (the scale bar is 10 μm long). (c) Molecular structure of the ionic liquid employed as electrolyte-gate dielectric. Both cation [P14]⁺ and anion [FAP]⁻ are shown. (d) Cross section of a WS_2 ionic liquid-gated FET.

A large area gold mesh and an oxidized Ag/AgO wire are used as gate electrode and quasi-reference electrode, respectively. When the gate electrode is biased, two electrical double layers are formed at the gate/electrolyte and semiconductor/electrolyte interfaces, enabling charge accumulation at the semiconductor surface.

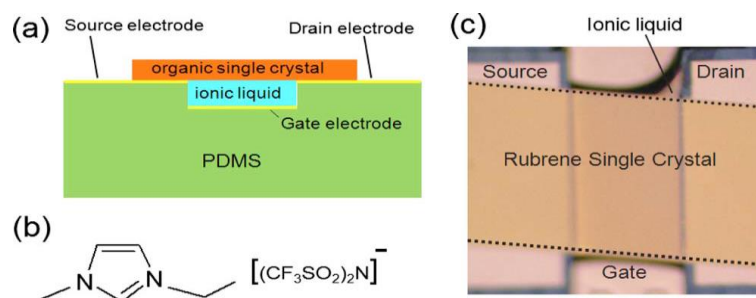


Fig. 11. (a)(b)Color online a structure of organic crystal/ionic liquid transistorsb emimTFSI. (c)Optical view of a rubrene crystal/emimTFS transistor.

4.2. Organic Semiconductor/Ionic Liquid Interface

Takeya's gathering as of now revealed another class of natural semiconductor gadgets functionalized by the quick ionic movement in the room temperature liquid salts. In this work, strong to-fluid interfaces are framed between natural semi-conductor single gems and ionic fluids so the structures fill in as quick exchanging natural field-effect transistors OFETs with the most elevated transconductance $gm = ID/VG$ per square channel sheet, i.e., the most proficient reaction of the yield channel current ID to the information door voltage VG among the OFETs at any point constructed. OFETs are possibility for cutting edge minimal effort de-indecencies that can be delivered by straightforward creation forms. There have been gives an account of the utilization of such polymer electrolytes as $LiClO_4$ disintegrated in polyethylene oxide or ionic fluid continued in a polymer gel.^{6–10} However, these gadgets experience the ill effects of either more unfortunate versatility or moderate reaction to VG as a result of generally moderate ionic dispersion in the polymer grid.

The OFETs are most regularly comprise of natural polycrystalline meager movies and dielectric protectors, for example, silicon dioxide. With common thicknesses of the door dielectric protectors of two or three hundred nanometers, many volts are expected to apply adequate EG for enough Q so down to earth flow intensification is accomplished. Takeya's gathering use RTILs for the door protecting layer and natural single precious stones for the semiconductor layer. The EDL capacitance of emimTFSI is estimated utilizing a test gadget comprising of the equivalent PDMS structure, where the top terminal is made out of gold slim movies. the EDL capacitance of the RTILs stays huge even at 1 MHz, showing the quick ionic dispersion because of the voltage application. Thusly, the EDL OFETs fusing the RTILs permit exchanging activity at such a high frequency. After presenting legitimate measures of RTIL, the fluid filled in the gap is continued steadily by the capillary force. Owing to the high charge carrier mobility in rubrene single crystals and the high capacitance of EDLs in the electrolyte, the device realizes the highest transconductance ever achieved for organic transistors.

5. Conclusion

I have surveyed in this article utilizations of semiconductor structure for the biosensor application by explicitly concentrating on the application as the detecting interface for the wide bio identification and therapeutic analysis. The quantity of productions on those points is extraordinarily expanding mirroring the solid interest for a clinical application. Because of trademark preproperties, for example, high affect ability, strength and unwavering quality, semiconductor seem to satisfy the solid need. In any case, for further improvement, explicit applications for which these particular application become novel (not effectively accomplished by other material) must be investigated. The In_2O_3 FET-put together wearable biosensors with respect to chip gold side entryway cathodes can be utilized for profoundly touchy recognition of glucose with a location limit down to 10 nm. In_2O_3 nanoribbon exhibits showed here will empower these applications and

extend minimal effort, huge region designing methodologies to empower an assortment of materials and structure geometries in nanoelectronics. Self-Assembled graphene Field-Effect Biosensors beats the coupling partiality subordinate affectability of nucleic corrosive biosensors and offers a pathway toward multiplexed and mark free nucleic corrosive testing with high precision and selectivity. Monolayer MoS₂ interface depicted interface here yield a wide accumulation of results identified with materials, gadget, and applications parts of the utilization of MoS₂ as separated precious stones and huge zone polycrystalline movies in biodegradable electronic frameworks. Membraneless FET Biosensors recommends a compelling stage for future touchy and reusable biosensors dependent on deformity free VDW materials. The upgraded PEC current acquired utilizing the wrinkled materials design empowered us to build up a delicate and mark free DNA biosensor with a picomolar limit-of-discovery [9]. GFETs defeats the coupling fondness subordinate affect ability of nucleic corrosive biosensors and offers a pathway toward multiplexed and mark free nucleic corrosive testing with high precision and selectivity. The significance of biodetection and clinical determination will upgrade much more later on. Despite the fact that solid requests for research and thought of semiconductor interesting properties, we will ready to recognize basic applications for the semiconductor [10].

Conflict of Interest

I guarantee that this paper is my original work and all the research results are unpublished. The authors declare no conflict of interest.

Author Contributions

The first author read the relevant documents, then analyzed and extracted the contents of the documents, and finally summarized the relevant contents and put them into paper.

Acknowledgment

The first author wishes to gratefully acknowledge assistant professor Zhe Wang for his guidance, patience and strong support.

References

- [1] Saha, S., Chan, Y., & Soleymani, L. (2018). Enhancing the photoelectrochemical response of DNA biosensors using wrinkled interfaces. *ACS Applied Materials & Interfaces*, 10(37), 31178-31185.
- [2] Woodhouse, M. & Goodrich, A. (2014). *A Manufacturing Cost Analysis Relevant to Single- and Dual-Junction Photovoltaic Cells Fabricated with III-Vs and III-Vs Grown on Czochralski Silicon* (Report No. NREL/PR-6A20-60126). US: National Renewable Energy Laboratory.
- [3] Kang, D., Young, J. L., Lim, H., Klein, W. E., Chen, H. D., Xi, Y. Z., *et al.* (2017). Printed assemblies of GaAs photoelectrodes with decoupled optical and reactive interfaces for unassisted solar water splitting. *Nat. Energy*, 2(5),17043.
- [4] Chen, X., Park, Y. J., Kang, M., Kang, S. K., Koo, J., Shinde, S. M., *et al.* (2018). CVD-grown monolayer MoS₂ in bioabsorbable electronics and biosensors. *Nat. Commun.*, 9(1), 1609.
- [5] Stebunov, Y. V., Yakubovsky, D. Y., Fedyanin, D. Y., Arsenin, A. V., & Volkov, V. S. (2018). Superior sensitivity of copper-based plasmonic biosensors. *Langmuir*, 34(15), 4681-4687.
- [6] Lee, H. W., Kang, D.-H., Cho, J. H., Lee, S., Jun, D.-H., & Park, J.-H. (2018). Highly sensitive and reusable membraneless field-effect transistor (FET)-type tungsten diselenide (WSe₂) biosensors. *ACS Applied Materials & Interfaces*, 10(21), 17639-17645.
- [7] Uemura, T., Hitahara, R., Tominari, Y., Ono, S., & Takeya, J. (2008). Electronic functionalization of solid-to-liquid interfaces between organic semiconductors and ionic liquids: Realization of very high

performance organic single-crystal transistors. *Appl. Phys. Lett.*, 93(26), 263305.

- [8] Braga, D., Lezama, I. G., Berger, H., & Morpurgo, A. F. (2012). Quantitative determination of the band gap of WS₂ with ambipolar ionic liquid-gated transistors. *Nano Lett.* 12(10), 5218-5223.
- [9] Liu, Q. Z., Liu, Y. H., Wu, F. Q., Cao, X., Li, Z., Alharbi, M., *et al.* (2018). Highly sensitive and wearable In₂O₃ nanoribbon transistor biosensors with integrated on-chip gate for glucose monitoring in body fluids. *ACS Nano*, 12(2), 1170-1178.
- [10] Zhao, C. Z., Xu, X. B., Bae, S. H., Yang, Q., Liu, W. F., Belling, J. N., *et al.* (2018). Large-area, ultrathin metal-oxide semiconductor nanoribbon arrays fabricated by chemical lift-off lithography. *Nano Lett.*, 18, 5590-5595.



Ming Rui Zhang was born on July 28, 1995 in Shenyang, Liaoning Province, China. He studied in Chongqing Jiaotong University from 2013 to 2017, majored in material physics, and obtained a bachelor's degree in 2017. The first author is currently studying for a master's degree in advanced engineering materials at the University of Manchester, UK. During the undergraduate and master's degree, the research field is mainly nano-materials.